Laser and Particle Beams

cambridge.org/lpb

Effects of wiggler error in a free-electron laser oscillator with two electron beams

Soon-Kwon Nam

Department of Physics, Kangwon National University, Chunchon 24341, Korea

Research Article

Cite this article: Nam S-K (2018). Effects of wiggler error in a free-electron laser oscillator with two electron beams. *Laser and Particle Beams* **36**, 448–453. https://doi.org/10.1017/S0263034618000459

Received: 20 June 2018
Accepted: 5 November 2018

Key words:
3D code; Two-beam; Wiggler error

Author for correspondence:
Soon-Kwon Nam, Department of Physics, Kangwon National University, Chunchon 24341, Korea, E-mail: snam@kangwon.ac.kr

Abstract

We have analyzed the effects of the wiggler error due to the electron beam's emittance, energy spreads, and higher-order modes in a free-electron laser (FEL) oscillator by using two electron beams of different energies based on the proposed FEL facility which is operated at a far-infrared and infrared regions. The three-dimensional (3D) effects in a FEL oscillator due to the wiggler error were calculated and an evaluation of the effect of the beam's emittance and energy spread was performed for the case of the coupled two-beam oscillator for phase shift errors and wiggler errors. The mode construction was studied on the higher-order modes of the wiggler for the various wiggler error parameters for FEL performance which is required for the high-quality electron beam. The radiation intensity at the fundamental mode was calculated for the rms phase shake in wiggler errors with sinus type, constant type, and parabolic type in the two-beam oscillator system using the 3D calculations. The results are compared with those of the fundamental modes without wiggler errors.

Introduction

In a free-electron laser (FEL) oscillator, the intensity of the radiation is reduced due to the optical diffraction and the instability of the electron beam. The FEL power depends on the electron beam stability, the optical diffraction, and three-dimensional (3D) effects. The stability of the electron beam (Nam and Kim, 2010) plays an important role in the electron beam and radiation field system and limit the operating wavelength, gain, and efficiency (Wang *et al.*, 2007) in the operation of a FEL.

McNeil *et al.*, proposed using a single pass in a two-beam FEL model (McNeil *et al.*, 2004). The model uses two electron beams with different energies in the 1D limit and shows an improved output coherence of the injected seed field. The higher energy electron beam is chosen so that its fundamental resonance wavelength is a harmonic resonance wavelength of the lower energy beam.

There are various error sources that might affect FEL operation such as beam steering errors, quadrupole alignment errors, wiggler alignment errors, wiggler imperfections (Freund and Jackson, 1994), and external ambient fields. These errors are external errors with respect to individual wiggler segments.

There are steering error and non-steering errors (Yu *et al.*, 1990). Steering errors induce small local kicks in the trajectory that reduce the overlap between the electron beam and the radiation field. Non-steering errors perturb the ponderomotive phase and induce the phase shake between the electron and the photon field. Both errors can significantly increase the saturation length and reduce the FEL power.

Steering errors are easily detected in the magnetic field measurements and these tolerances can be compensated using shimming and tuning procedures in a straightforward manner.

In this paper, we have developed a code using an extended 3D model with two electron beams that include wiggler errors, the electron beam's emittance, energy spread, and higher-order modes. The evolution of the radiation field intensity for the fundamental and higher-order modes for the various wiggler errors is studied.

The effects of the wiggler errors for a proposed FEL facility that will be operated in the far-infrared and infrared region at cyclotron research institute were studied by using an extended 3D simulation code that we have developed

The paper also presents the normalized FEL amplitude for the optimization of the beam's emittance and energy spread due to the wiggler errors. The effects of the higher order modes due to the wiggler error for emittance and energy spread in the coupled two-beam oscillator system.

The model and numerical simulation

Errors in wiggler magnetic field and electron beam steering can degrade the FEL performance.

We will assume that each wiggler segment is shimmed to have vanishing first and second magnetic field integrals and focus on the variations of the wiggler parameter K due to magnetic field errors or transverse misalignments among segments. Using the 1D FEL equations, Yu and Krinsky, studied the effect of wiggler errors (Yu and Krinsky, 1992) on FEL performance.

When the undulator strength parameter has an error $\Delta K = K - K_0$, the phase change (Huang and Kim, 2007) can be written as

$$\frac{d\theta}{dz} = k_u - k_s \frac{1 + ((K_0 + \Delta K)^2/2)}{2\gamma^2} \approx 2k_u - k_u \frac{K_0 \Delta K}{1 + (K_0^2/2)}. \quad (1)$$

Here, the first term describes the ideal motion, and the second term is the amount of the phase kick due to small changes in K.

We have introduced a magnetic correlation length $L_c = N_c \lambda_u$ which is assumed to be much shorter than the approximate field amplitude gain length. Then the net phase shift per gain length is

$$\Delta\theta = \sum_{n=1}^{2L_{3G}/L_c} N_c \frac{2\pi K_0 \Delta K_n}{1 + K_0^2/2}, \quad (2)$$

For $2\ L_{3G}/L_c \gg 1$, $\Delta\theta$ has a zero mean and a variance

$$< (\Delta\theta)^2 > = \frac{L_{3G}}{L_c} \left(N_c \frac{2\pi K_0^2}{1 + (K_0^2/2)} \frac{\sigma_K}{K_0} \right)^2. \quad (3)$$

where σ_K is the rms value of ΔK_n.

The 3D gain length (Xie, 2000) of a FEL has expressed as

$$L_{3G} = L_{1g}(1 + \Lambda). \quad (4)$$

The correction factor Λ has been obtained by 3D numerical studies.

$$\Lambda = F(X_\gamma, X_d, X_\varepsilon) \quad (5)$$

where,

$$X_\gamma = 4\pi \frac{L_{1g}}{\lambda_w} \frac{\sigma_\gamma}{\gamma}, \quad X_d = \frac{L_{1g}}{L_r}, \quad X_\varepsilon = \frac{L_{1g}}{\beta} \frac{4\pi\varepsilon}{\lambda} \quad (6)$$

with σ_γ is the energy spread, and ε is the emittance.

$$L_r = \frac{\pi w_0^2}{\lambda}. \quad (7)$$

L_r is the Rayleigh range.

The extended 3D equations describing the effect of the wiggler errors due to the phase shift, the 3D gain length, energy spread, and emittance in FEL interaction of the lower and higher energy electron beams with oscillator may be written as

$$\frac{d\vartheta[x,y,\bar{z}]_j}{d\bar{z}} = [\gamma[x,y,\bar{z}]_j - \gamma_r[x,y,\bar{z}]] + k_s \varepsilon_n/2 \overline{\gamma_1} k_u \overline{\rho_1} \bar{\beta}, \quad (8)$$

$$\frac{d\varphi[x,y,\bar{z}]_j}{d\bar{z}} = [\Gamma[x,y,\bar{z}]_j - \Gamma_r[x,y,\bar{z}]] + k_s \varepsilon_n/2\overline{\gamma_n} k_u \overline{\rho_n} \bar{\beta}, \quad (9)$$

The scaled lower and higher electron-energy parameters in the phase Eqs (8) and (9) are defined as

$$\gamma[x,y,\bar{z}]_j \equiv (\gamma_j - \overline{\gamma_1})/\ \overline{\rho_1}\ \overline{\gamma_1} \quad (10)$$

$$\Gamma[x,y,\bar{z}]_j \equiv (\gamma_j - \overline{\gamma_n})/\overline{\rho_n}\ \overline{\gamma_n} \quad (11)$$

with the relation $\overline{\gamma_n} = \sqrt{n}\,\overline{\gamma_1}$, and the normalized emittance of ε_n.

The coupling of the lower-energy electrons to both the fundamental and the harmonic fields are seen in Eq. (12). From Eq. (13), the higher-energy electron couples only to the harmonic field A_H (its fundamental field).

$$\frac{d\gamma[[x,y,\bar{z}]_j}{d\bar{z}} = -\sum_{h.odd}^{n} F_h (A_L e^{ih\vartheta[x,y,\bar{z}]_j} + c.c.), \quad (12)$$

$$\frac{d\Gamma[x,y,\bar{z}]_j}{d\bar{z}} = -c_1 F_1 (A_H e^{ih\vartheta[x,y,\bar{z}]_j} + c.c.), \quad (13)$$

where $j = 1,\ldots, N$ are the total number of electrons, $h = 1, 3, 5, \ldots$ are the odd harmonic components of the field, and $F_{h,k}$ are the usual differences of Bessel function factors.

The field A_L is seen from Eq. (14) to be driven only by the lower energy electron beam. Equation (15) demonstrates that the harmonic field has two driving sources: The lower and higher energy electron beams.

$$\left(\frac{\partial^2}{\partial x^2} + \frac{\partial^2}{\partial y^2} + 2i\, k_s \frac{\partial}{\partial \bar{z}}\right) A_L[x,y,\bar{z}] = S_{h\vartheta}, \quad (14)$$

$$\left(\frac{\partial^2}{\partial x^2} + \frac{\partial^2}{\partial y^2} + 2i\, k_s \frac{\partial}{\partial \bar{z}}\right) A_H[x,y,\bar{z}] = (S_\varphi + S_{n\vartheta}), \quad (15)$$

where

$$S_{h\vartheta} = F_k e^{-ik\vartheta[x,y,\bar{z}]}, \quad (16)$$

$$S_\varphi = c_2 F_1 e^{-i\varphi[x,y,\bar{z}]}, \quad (17)$$

$$c_1 = \frac{1}{n^{1/4}} \left(\frac{\rho_n}{\rho_1}\right)^{3/2}, \quad (18)$$

$$c_2 = n^{1/4} \left(\frac{\rho_n}{\rho_1}\right)^{3/2}, \quad (19)$$

$$\bar{z} = 2k_u \rho z, \quad (20)$$

https://doi.org/10.1017/S0263034618000459 Published online by Cambridge University Press

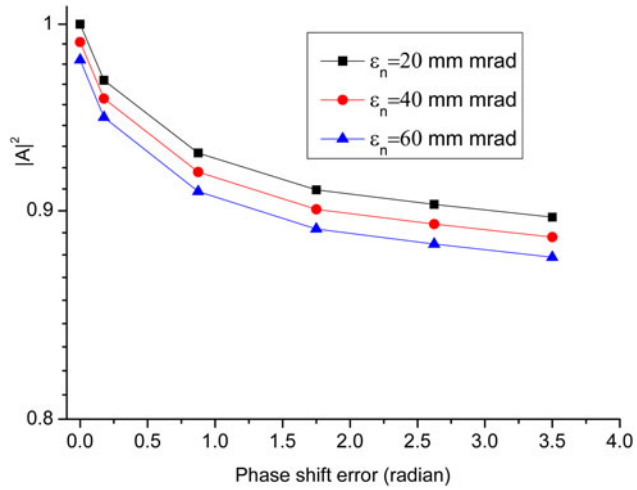

Fig. 1. Evolution of the harmonic radiation field intensity, for varying emittance of 20, 40, and 60 mm·mrad, for a phase shift errors of 0–4 radian (both beams).

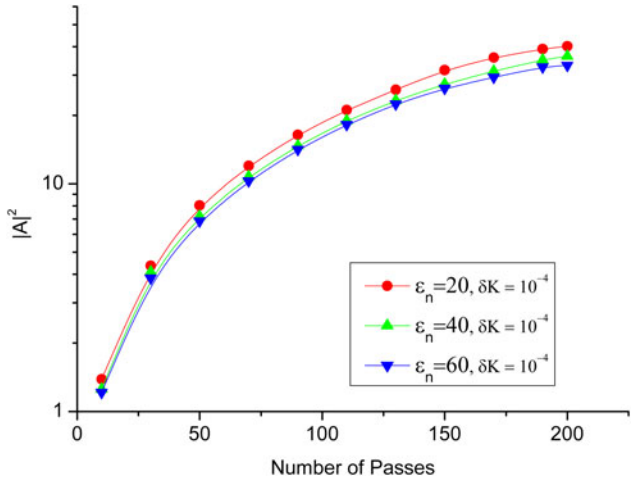

Fig. 2. Evolution of the harmonic radiation field intensity, for varying emittance of 20, 40, and 60 mm·mrad, for a wiggler error of $\Delta K = 10^{-4}$ (both beams).

where, h refers to all odd harmonics $h < n$, I is the beam current, and the subscripts 1 (n) refer to the parameters of the lower (higher) energy beam.

The analysis of the system has been carried out using the method of numerical simulations with collective variables (Bonifacio and McNeil 1988; Bonifacio *et al.*, 1984).

The parameters of our simulation were wiggler period 2.5 cm; a number of periods of 80; beam currents (I_b) 75 and 25 A for $n = 3$ and 5, respectively; curvature radius of 450 ~ 520 cm; and a resonator length of 8.0 m. The simulation used our extended 3D simulation code, which describes the effects of two-electron beams with different energies, that is, 13.4 MeV (higher beam) and 6 MeV (lower beam). The seed field at the lower electron beam energy is modeled by defining its initial scaled intensity at the beginning of the FEL interaction $|A_{L1}(\bar{z} = 0)|^2 = (1 + I)\ \exp[-(x^2 + y^2)/0.5] \times 10^{-8}$ to be two orders of magnitude greater than that of the harmonic. The multi-particle and multi-pass simulations were performed for a particle number of 300 and a pass number of 200. In the simulations, the minimum waist position of the radiation is at the center of the cavity. The radiation spot size (w_0) at the minimum waist, higher harmonics (k, $n = 3$ and 5) and the number of macro-particles ($j = 300$) were used in the simulation.

An evaluation of the effect of the beam's emittance was performed for the case of the coupled two-beam oscillator with a phase shift errors 0–4 radian as shown in Figure 1. For the maximum emittance of the higher beam at $\epsilon_n = 60$ mm · mrad, the saturation intensity $|A|^2$decreases by approximately 3% relative to those of the minimal emittances of $\epsilon_n = 20$ mm · mrad of the two-beam system as shown in Figure 1. However, the harmonic field intensity of both beams with phase shift errors is decreased significantly compared with that of both electron beam without phase shift errors for varying emittances and it was decreased by approximately 11% in the case of both beams with phase shift errors.

An evaluation of the effect of the beam's emittance was performed for the case of the coupled two-beam oscillator with for a wiggler error of $\Delta K = 10^{-4}$ as shown in Figure 2. For the maximum emittance of the higher beam at $\epsilon_n = 60$ mm · mrad, the saturation intensity $|A|^2$decreases by approximately 9% for $n = 3$ relative to those of the minimal emittances of $\epsilon_n = 20$ mm · mrad of the two-beam system as shown in Figure 2.

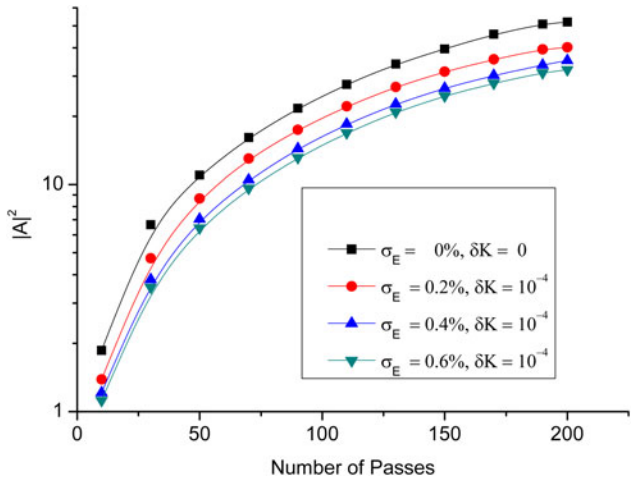

Fig. 3. Evolution of the maximum harmonic intensity in the two-beam oscillator for Gaussian energy spreads from $\sigma_E = 0$ to $\sigma_E = 0.6\%$ in the higher energy beam with and without wiggler errors.

Figure 3 shows the evolution of the harmonic intensity for the case of the coupled two-beam oscillator with and without wiggler errors for varying Gaussian energy spreads σ_E.

For an energy spread of the higher beam of $\sigma_E = 0.6\%$ for the case of the coupled two-beam oscillator with wiggler errors, the saturation intensity $|A|^2$ decreases by approximately 11% relative to that of the energy spread of $\sigma_E = 0.2\%$ the higher beam as shown in Figure 3.

However, for an energy spread of $\sigma_E = 0.6$ % for the case of both beam with wiggler error of $\delta K = 10^{-4}$, the saturation intensity $|A|^2$ decreases significantly by 23% relative to that of both beam without energy spread and without wiggler error.

The field distribution of 3D Hermite-Gaussian beams (Wu and Lu, 2002) for the higher-order modes is described at the plane $z_0 = 0$ as:

$$A_{m,n}(x_0, y_0, z_0 = 0) = H_m\left(\frac{x_0}{w_{0x}}\right) H_n\left(\frac{y_0}{w_{0y}}\right) \exp\left[-\left(\frac{x_0^2}{w_{0x}^2} + \frac{y_0^2}{w_{0y}^2}\right)\right] \quad (21)$$

https://doi.org/10.1017/S0263034618000459 Published online by Cambridge University Press

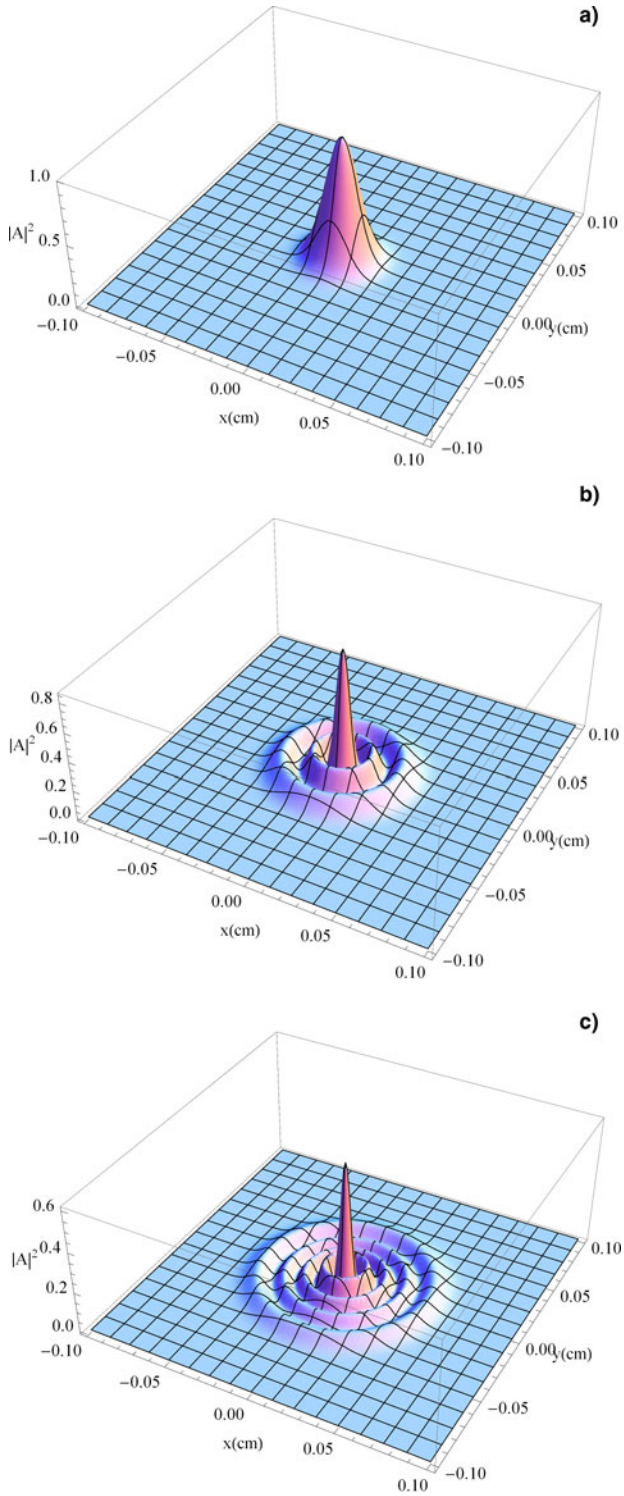

Fig. 4. (Color online) Evolution of the radiation field intensity $|A|^2$ for the (a) fundamental, (b) 3rd-, and (c) 5th-order modes for wiggler error dk = 0.0 without an emittance and without energy spread.

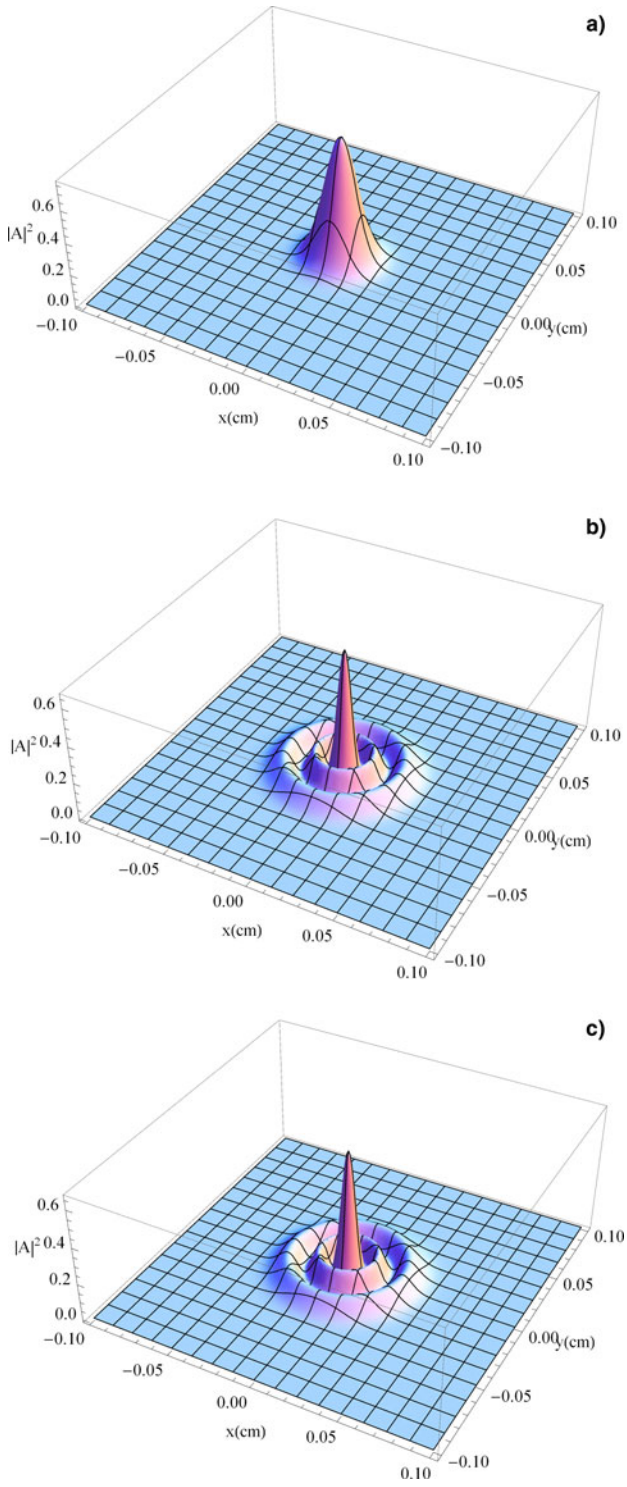

Fig. 5. (Color online) Evolution of the radiation field intensity $|A|^2$ for the (a) fundamental, (b) 3rd-, and (c) 5th-order modes for wiggler error dk = 0.0001 with an emittance of $\varepsilon_n = 10$ mm · mrad and energy spread of 0.3%.

where H_m and H_n denotes the Hermite polynomial of order m and n, w_{0x} and w_{0y} are waist widths in the x and y-direction, respectively.

The field error is assumed to be much smaller than the field itself, $\Delta K < K_0$, where ΔK and K_0 denote the maximum error amplitude and the nominal value of the undulator parameter, respectively. The phase error (Li *et al.*, 2008) for periodic errors on phase shake is

$$\delta\theta = \frac{k_u}{1 + K_0^2} \int_0^z 2K_0 \Delta K f(z')\mathrm{d}z' . \quad (22)$$

https://doi.org/10.1017/S0263034618000459 Published online by Cambridge University Press

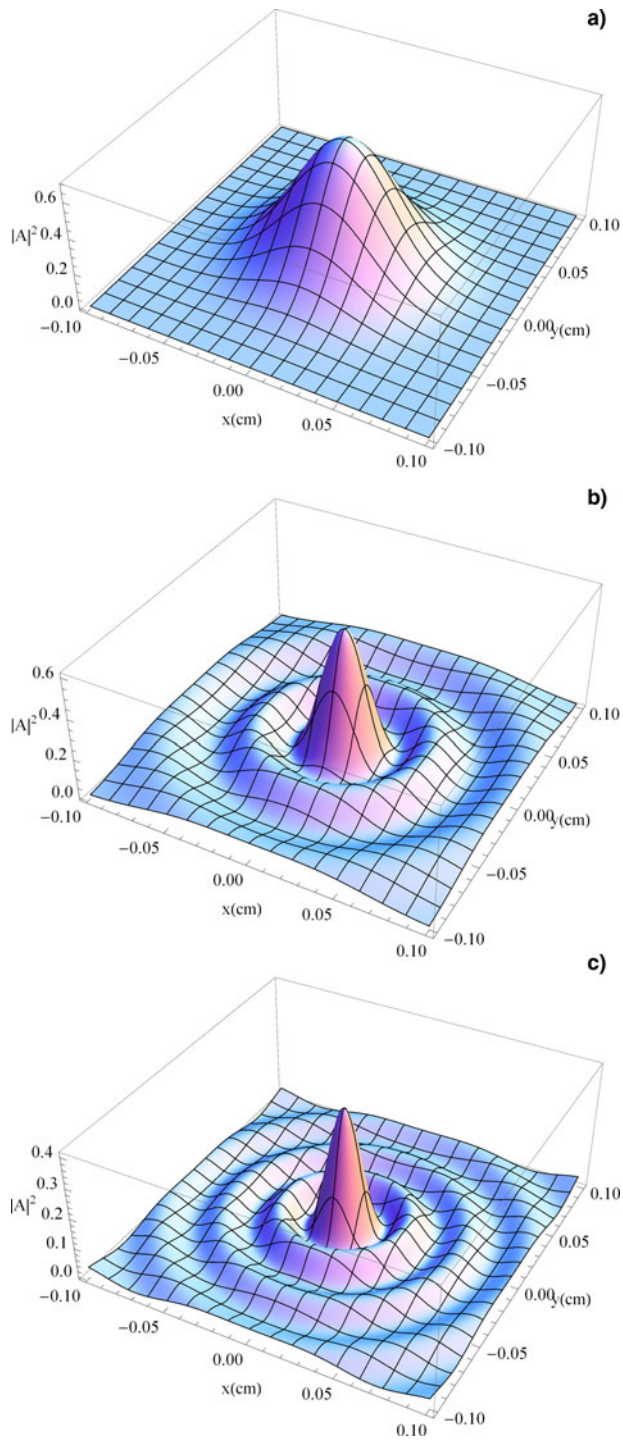

Fig. 6. (Color online) Evolution of the radiation field intensity $|A|^2$ for the (a) fundamental, (b) 3rd-, and (c) 5th-order modes for wiggler error dk = 0.0001 with an emittance of $\varepsilon_n = 30$ mm · mrad and energy spread of 0.5%.

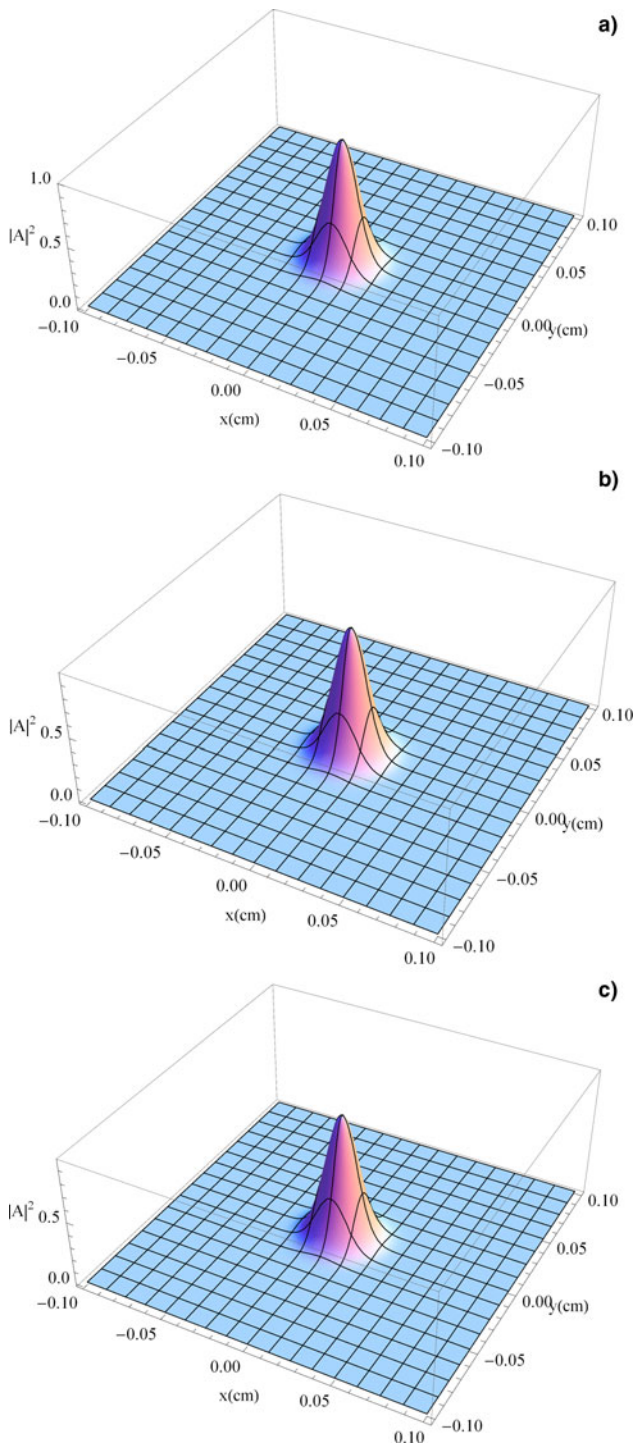

Fig. 7. (Color online) Evolution of the radiation field intensity $|A|^2$ for rms phase shake error with sinus type (a), with constant type (b), and with parabolic type (c) for without an emittance and without energy spread.

where $f(z)$ describes the error shape, $|f(z)| \leq 1$. $f(z)$ is a periodic function with periodic length λ_δ and $f(z) = f(z + \lambda_\delta)$. If z is normalized, $z_n = z/\lambda_\delta$.

$$\delta\theta = \frac{k_u}{1+K_0^2} 2K_0 \Delta K \lambda_\delta \int_0^{z_n} f(z_n') dz_n' = \frac{2k_u K_0^2}{1+K_0^2} \frac{\Delta K}{K_0} \lambda_\delta g(z_n) \quad (23)$$

Since the error function is periodic, the integration can be restricted to one error period length and a SASE-FEL always radiates at a wavelength for which $<\delta\theta> = 0$.

Therefore the rms phase shake is given by

$$\sigma_{\delta\theta} = \frac{2k_u K_0^2}{1+K_0^2} \frac{\Delta K}{K_0} \lambda_\delta \sqrt{\int_0^1 g^2(z_n) dz_n} = \alpha \frac{2k_u K_0^2}{1+K_0^2} \frac{\Delta K}{K_0} \lambda_\delta. \quad (24)$$

https://doi.org/10.1017/S0263034618000459 Published online by Cambridge University Press

This equation is valid for all kinds of periodic errors. Different gap profiles are described by the coefficient α. The strength is given by ΔK.

The radiation amplitudes of the 1st-order, 3rd-order, and 5th-order for the wiggler error with an emittance of ε_n =10, 20, and 30mm·mradand energy spread of 0 ∼ 0.5% in the two-beam oscillator system are shown in Figures 4–6, respectively. The higher-order modes have lower radiation amplitudes relative to the fundamental mode in the higher energy beam with the wiggler error, emittance, and energy spread.

For wiggler error $\Delta K = 0.0001$ with an emittance of $\varepsilon_n = 30\text{mm} \cdot \text{mradand}$ energy spread of 0.5% in the two-beam oscillator system, the saturation intensity $|A|^2$ at the fundamental mode decreased by 31% in the 3D simulation relative to those of the fundamental modes for the wiggler error $\Delta K = 0.0$ without an emittance and without energy spread in the two-beam oscillator system.

However, for the rms phase shake in wiggler errors with sinus ($\alpha = 0.113$), constant ($\alpha = 0.144$) and parabolic type ($\alpha = 0.970$) in the two-beam oscillator system, the saturation intensity $|A|^2$ at the fundamental mode decreased by approximately 4% only in the 3D calculations relative to those of the fundamental modes without wiggler errors for the case without an emittance and without energy spread as shown in Figure 7.

Conclusions

An evaluation of the effect of the diffraction parameters was performed using an extended 3D FEL code with two electron beams that we have developed.

An evaluation of the effect of the beam's emittance was performed for the case of the coupled two-beam oscillator with a phase shift errors. The harmonic field intensity of both beams with phase shift errors was decreased significantly compared with that of both electron beam without phase shift errors for varying emittances.

For the maximum emittance of the higher beam at $\varepsilon_n = 60\ \text{mm} \cdot \text{mrad}$, the saturation intensity was decreased by approximately 9% relative to those of the minimal emittances of $\varepsilon_n = 20\ \text{mm} \cdot \text{mrad}$ for a wiggler error of $\Delta K = 10^{-4}$ of the two-beam system. For an energy spread of the higher beam of $\sigma_E = 0.6\%$ for the case of the coupled two-beam oscillator with wiggler errors, the saturation intensity $|A|^2$ was decreased by approximately 11% relative to that of the minimal energy spread of $\sigma_E = 0.2\%$.

However, for an energy spread of $\sigma_E = 0.6$ % for the case of both beam with wiggler error of $\delta K = 10^{-4}$, the saturation intensity $|A|^2$ was decreased significantly by 23% relative to that of both beam without energy spread and without wiggler error.

The radiation field intensity for the higher order modes was highly sensitive to the wiggler error for the energy spread but less sensitive to the wiggler error for the emittance in the coupled two-beam oscillator. For wiggler error with an emittance and energy spread, the saturation intensity $|A|^2$ at the fundamental mode was highly sensitive in the 3D simulation relative to those of the fundamental modes without wiggler error for without emittance and without energy spread in the two-beam oscillator system. However, for the rms phase shake in wiggler errors with sinus, constant and parabolic type, the saturation intensity $|A|^2$ at the fundamental mode was not sensitive in the 3D calculations relative to those of the fundamental modes without wiggler errors for the case without energy spread and without emittance.

Acknowledgments. This research was supported by Basic Science Research Program through the National Research Foundation of Korea (NRF) funded by the Ministry of Science (NRF-2017R1A2B4002015).

References

Bonifacio R and McNeil BWJ (1988) Slippage and superradiance in the high-gain FEL. *Nuclear Instruments & Methods in Physics Research, Section A: Accelerators, Spectrometers, Detectors, and Associated Equipment* **272**, 280.

Bonifacio R, Pelligrini C and Narducci LM (1984) Collective instabilities and high-gain regime in a free electron laser. *Optics Communications* **50**, 373.

Freund HP and Jackson RH (1994) Wiggler imperfections in free-electron lasers. *Nuclear Instruments and Methods in Physics Research Section A* **341**, 225–229.

Huang Z and Kim KJ (2007) Review of x-ray free-electron laser theory. *Physical Review Accelerators and Beams* **10**, 034801.

Li Y, Faatz B and Pflueger J (2008) Undulator system tolerance analysis for the European x-ray free-electron laser. *Physical Review Accelerators and Beams* **11**, 100701.

McNeil BWJ, Robb GRM and Poole MW (2004) Two-beam free-electron laser. *Physical Review E*, **70**, 035501.

Nam S and Kim K (2010) Stability of an electron beam in a two-frequency wiggler with a self-generated field. *Journal of Plasma Physics*, **77**, 257.

Wang XJ, Watanabe T, Shen Y, Li RK, Murphy JB, Tsang T and Freund HP (2007) Efficiency enhancement using electron energy detuning in a laser seeded free electron laser amplifier. *Applied Physics Letters* **91**, 181115.

Wu P and Lu B (2002) Propagation of three-dimensional elegant Hermite-Gaussian beam through a 4 × 4 paraxial optical system. *Optik*. **113**, 245.

Xie M (2000) Exact and variational solutions of 3D eigenmodes in high gain FELs. *Nuclear Instruments & Methods in Physics Research, Section A: Accelerators, Spectrometers, Detectors, and Associated Equipment* **445**, 59.

Yu LH and Krinsky S (1992) Effect of wiggler errors on free electron-laser gain. *Physical Review A* **45**, 1163.

Yu LH, Krinski S and Gluckstern R (1990) Calculation of universal scaling function for free-electron-laser gain. *Physical Review Letters* **64**, 3011.

https://doi.org/10.1017/S0263034618000459 Published online by Cambridge University Press